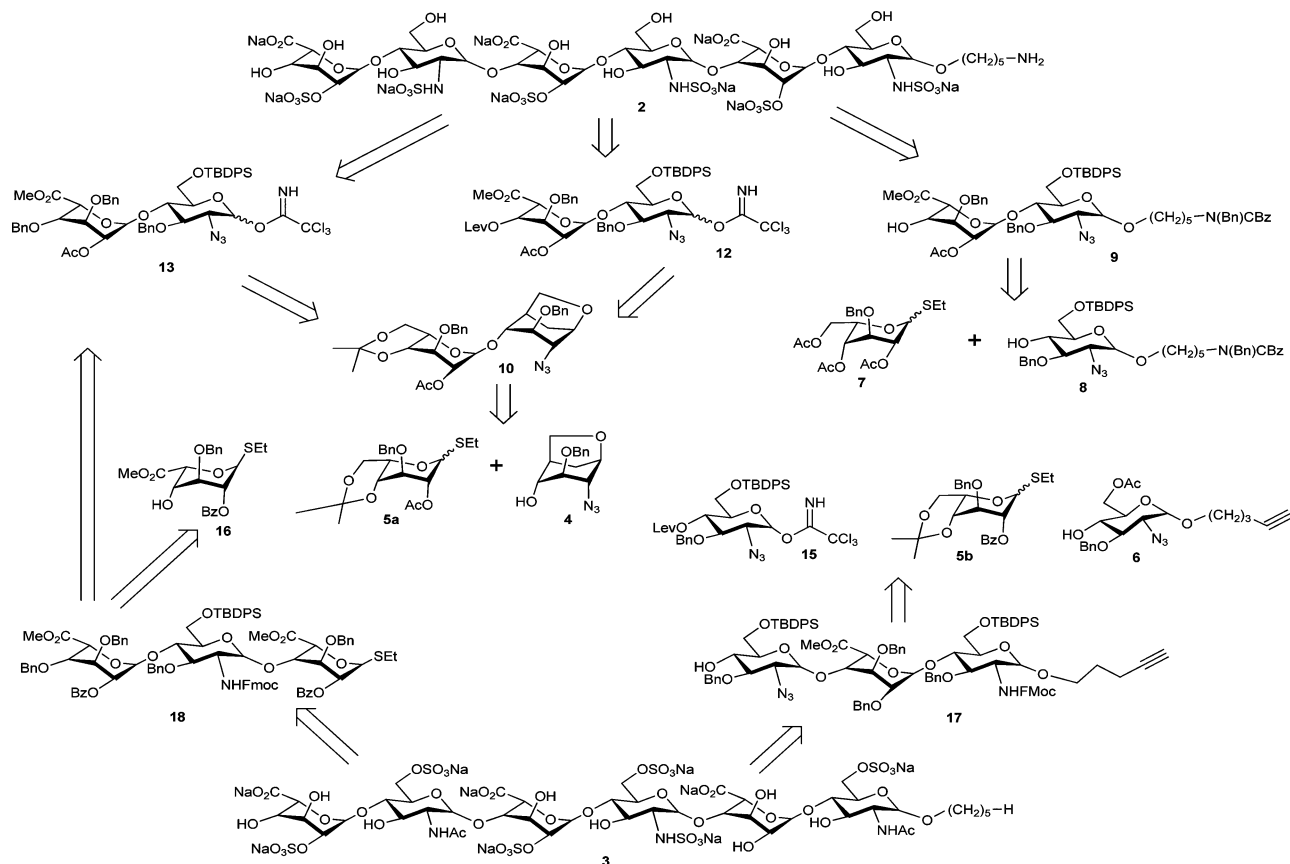


Figure 1. Structures of hexasaccharides 1–3.

Scheme 1. Retrosynthetic Route for the Synthesis of Hexasaccharides 2 and 3



further evaluated *in vitro* for their affinity for these protein targets, as well as heparanase inhibition.

The hexasaccharides contain the same (L-iduronic acid-D-glucosamine)₃ carbohydrate backbone but varying substitution patterns. The synthesis of compound 1 via another route has been reported by Petitou and co-workers.¹⁸ We present here a new synthesis of 2, the β isomer having been described previously by Seeberger and co-workers,¹⁷ and a concise synthesis of the irregular α -pentyl hexasaccharide 3.

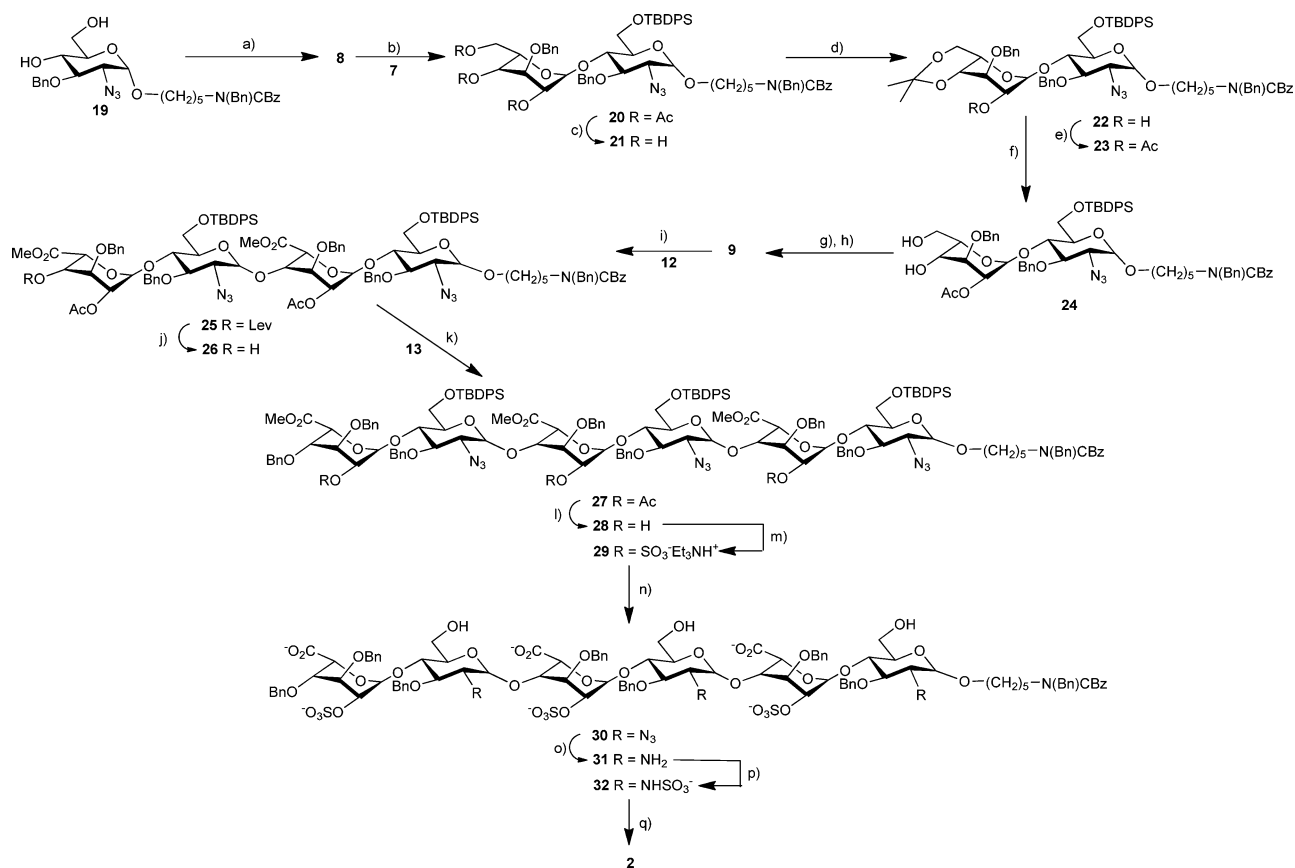
RESULTS AND DISCUSSION

Although the chemical synthesis of the regular sequences appearing in H/HS, particularly the IdoA_{2S}-Glc_{NS,6S} disaccharide (Glc_{NS,6S} represents N- and 6-O-sulfonated glucosamine), has been well-documented,^{19–24} the preparation of such structures is often tedious and challenging.

The major concerns in the preparation of 1–3 involve the backbone assembly: regio- and stereochemical control in

glycosidic bond formation, the different functional makeup of the amino groups (NH₂, NHSO₃Na, and NHAc), followed by the introduction of sulfate ester groups at specific positions. More so, the synthesis of irregular structures such as 3 presents a difficult task, with the successful synthesis of an irregular octasaccharide being reported only recently.²⁵ Despite the similarity of the three hexasaccharide templates, minor changes in the sulfation/acetylation pattern proved to have a significant impact on the synthesis route. It was observed that simply introducing one nonsulfated uronic acid accompanied by an N-sulfo glucosamine residue in 3 proved to be a formidable synthesis exercise compared to the synthesis of 1 or 2. Herein, we have proposed efficient solutions for the backbone construction and the control of stereochemistry in each case and attempted to study the influence of the targeted substitution pattern on their bioactivity profiles.

Synthesis of 1. Preparation of N-acetylated hexasaccharide 1 is today a classic exercise²⁶ after the description of several

Scheme 2. Synthesis of Hexasaccharide 2^a

^aReagents and conditions: (a) TBDPSCl, Et₃N, DMAP, CH₂Cl₂, RT, 88%; (b) NIS, TfOH, CH₂Cl₂, 4 Å molecular sieves, 0 °C, 80%; (c) CH₃ONa, CH₃OH/THF, RT; (d) (CH₃O)₂C(CH₃)₂, CSA, DMF, RT; (e) Ac₂O, Et₃N, DMAP, CH₂Cl₂, RT; (f) 60% AcOH, THF, 80 °C; (g) TEMPO, bromodan, CH₃CN/aqueous NaHCO₃, RT; (h) CH₃I, NaHCO₃, DMF, RT overnight, 23% overall yield for steps c–h; (i) TBDMSOTf, toluene, 4 Å molecular sieves, –20 to 0 °C, 91%; (j) NH₂NH₂/AcOH, pyridine/AcOH (75/25), RT, 75%; (k) TBDMSOTf, toluene, 4 Å molecular sieves, –20 to 0 °C, 80%; (l) K₂CO₃, MeOH, RT; (m) Py·SO₃, pyridine, 55 °C; (n) (1) NH₄F, MeOH, 50 °C, (2) 0.7 M LiOH, MeOH, RT, 64% overall yield for steps l–n; (o) propanedithiol, Et₃N, MeOH, RT, 92%; (p) Py·SO₃, Na₂CO₃, aqueous NaHCO₃, 0 °C, 75%; (q) H₂, 10% Pd/C and Pd(OH)₂, H₂O, RT, 87%.

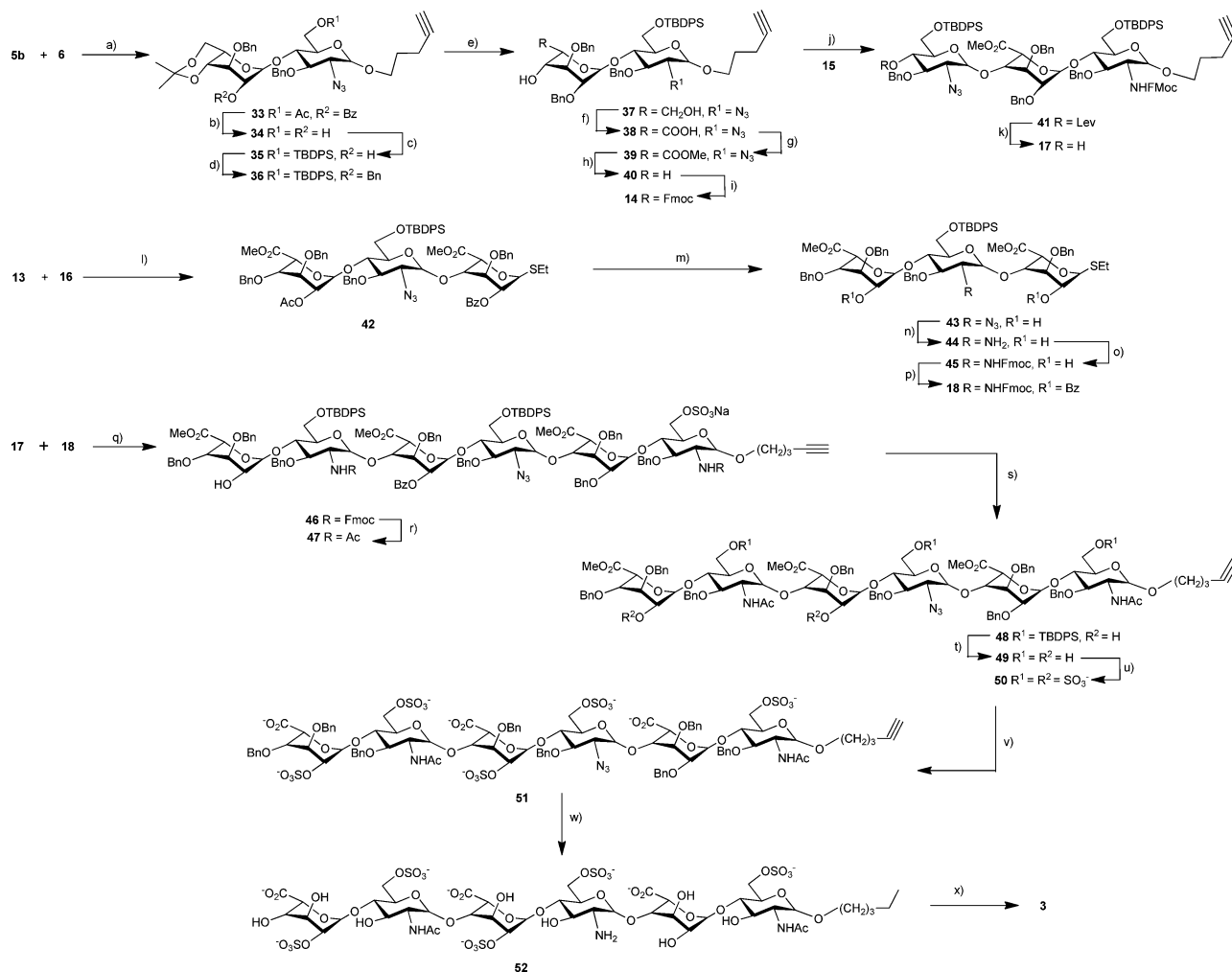
routes toward *N*-sulfated analogues, the so-called “regular region of heparin”. Thus, **1** was obtained after selective acetylation of its triamino precursor resulting from a classical disaccharide building-block approach.^{21,27} Several similar *N*-acetylated oligosaccharides that differ from **1** by the nature of the aglycon have been previously reported.^{17,28} In the case presented here, the pentenyl moiety was originally introduced at the anomeric position of the monosaccharide unit to allow further functionalization. Fortunately, the pentenyl aglycon afforded easier separation of the α and β isomers during the preparation of the reducing end monosaccharide.

Synthesis of 2. The route to hexasaccharide **2** is outlined in Schemes 1 and 2. The difficulty in the synthesis of this compound was caused by the presence of the free amine that was introduced in the aglycon to allow further modification. This required the use of an amino protecting group orthogonal to the protecting group used at the 2*N*-position of the glucosamine units. An efficient solution was obtained by using the benzyloxycarbonylated protected amine **8** as described in previous reports on heparin oligosaccharide synthesis.^{17,29} Conversely, azido groups were used as protecting groups for later conversion to *N*-sulfates without affecting the protection of the other primary amine, *N*-(Bn)CBz, present on the aglycon, which was successfully deprotected later by catalytic

hydrogenation. During this synthesis, a TBDPS group was employed as the permanent protecting group of the glucosamine primary alcohols.

Three building blocks (**9**, **12**, and **13**) were required for the synthesis of **2**. For the preparation of imidates **12** and **13**, known monosaccharides **4** and **5a** were condensed to give **10**, which was converted to the desired imidate using a classical series of reactions.¹⁸ Reducing end disaccharide **9** was prepared (Scheme 2) from monosaccharides **7** and **8** (prepared from **19**) as described by Boons.³⁰

The assembly of hexasaccharide **27** was thus accomplished using disaccharide units **9**, **12**, and **13** as outlined in Scheme 2. Coupling of **9** and **12** afforded fully protected tetrasaccharide **25**. Removal of the levulinoyl group at C4 and coupling with **13** resulted in hexasaccharide **27**. Deacetylation using K₂CO₃ gave **28** in quantitative yield followed by *O*-sulfation using the pyridine–sulfur trioxide complex in pyridine, cleavage of *O*-silyl groups at position 6, and hydrolysis of ester groups to afford **30**. The azido groups of **30** were subsequently reduced to amines using propanedithiol and then subjected to *N*-sulfation using the pyridine–sulfur trioxide complex to afford **32**. Hydrogenolysis of **32** using H₂ in the presence of Pd catalyst afforded **2**.

Scheme 3. Synthesis of Hexasaccharide 3^a

^aReagents and conditions: (a) NIS, TfOH, CH₂Cl₂, 4 Å molecular sieves, 0 °C, 68%; (b) 0.5 M MeONa, MeOH, RT, 1 h, 55%; (c) TBDPSCI, Et₃N, DMAP, CH₂Cl₂, RT; (d) BnBr, NaH, DMF, RT, 12 h, 84% overall yield for steps c and d; (e) 80% aqueous AcOH/THF (7/3), 80 °C; (f) TEMPO, BAIB, CH₂Cl₂, H₂O, RT; (g) MeI, NaHCO₃, DMF, RT, overnight, 69% overall yield for steps e–g; (h) propanedithiol, Et₃N, CH₃OH, 45 °C, 83%; (i) Fmoc-Cl, DIPEA, CH₂Cl₂, 4 °C, 71%; (j) TBDMSOTf, 4 Å molecular sieves, CH₂Cl₂, –20 °C, 53%; (k) NH₂-NH₂, AcOH, pyridine, RT, 83%; (l) TBDMSOTf, 4 Å molecular sieves, CH₂Cl₂, –20 °C, 61%; (m) K₂CO₃, MeOH/THF (7/3), RT, 81%; (n) propanedithiol, MeOH, Et₃N, RT, 90%; (o) Fmoc-Cl, CH₂Cl₂, DIPEA, 4 °C, 76%; (p) BzCl, pyridine, RT, 2 h, 86%; (q) NIS, TfOH, 4 Å molecular sieves, CH₂Cl₂, –20 °C to RT, ~22%; (r) piperidine, DMF, Ac₂O, RT, 90%; (s) MeONa, MeOH/THF (4/1), RT, 89%; (t) HF-Py, pyridine, TMSOMe, RT, >99%; (u) Py-SO₃, pyridine, MeOH, Et₃N, 55 °C, 88%; (v) LiOH, H₂O, 40 °C, 33%; (w) Pd(OH)₂, H₂, H₂O, RT, 69%; (x) Py-SO₃, saturated aqueous NaHCO₃, Na₂CO₃, 0 °C, 95%.

Synthesis of 3. As mentioned before, the challenge in the synthesis of hexasaccharide 3 arose from its “irregular structure” and the presence of *N*-acetylated and *N*-sulfated *D*-glucosamines and one nonsulfated uronic acid unit. We successfully devised the route outlined in Scheme 3 in which the key glycosylation reaction connects two trisaccharide building blocks bearing differential *N*-protected glucosamine precursors. Thus, the stereoselectivity of the last created glycosidic bond was secured by the adjacent benzoyl groups via neighboring group participation. An additional key reaction was the selective reduction of the azido group on the hexasaccharide in the presence of the Fmoc group using propanedithiol and triethylamine in methanol.

Having tested the key steps of the process, we embarked on the synthesis of 46, the fully protected hexasaccharide precursor of 3. Disaccharide 33 obtained by coupling 5b¹⁸ and 6¹⁸ was converted into 14 following a classical series of reactions,

including the reduction of the azido group with propanedithiol followed by protection as an Fmoc carbamate. Reaction of 14 with imidate 15^{18,31} led to trisaccharide 41, and subsequent removal of the levulinoyl group gave glycosyl acceptor 17. The synthesis of the second trisaccharide required the preparation of acceptor monosaccharide 16, which was obtained by the oxidation of the primary alcohol derivative, followed by esterification of the carboxylic acid, as reported by Tabeur et al.³¹ Reaction of 16 with disaccharide imidate 13 gave trisaccharide 18 after a series of routine protecting group manipulations.

Compound 17 was condensed with glycosyl donor 18 to obtain the desired hexasaccharide template 46 (Scheme 3), which was subsequently subjected to a series of functional group transformations to obtain fully functionalized hexasaccharide 3. Replacement of the Fmoc protecting group in 46 with an acetyl group using acetic anhydride in a DMF/

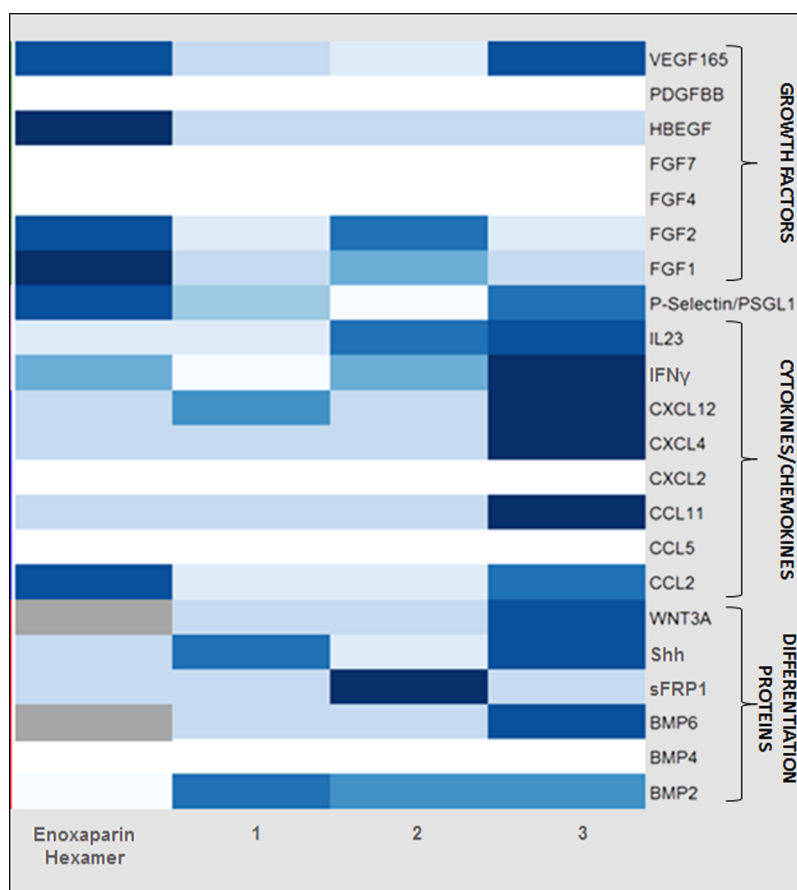


Figure 2. Heat map depicting the affinities of 1–3 compared to those of the enoxaparin hexamer mixture for a panel of 22 selected HBPs as measured by K_D (nanograms per milliliter). Inhibition of PSEL/PSGL1 interaction by the test compounds is expressed as K_i values. Darker colors indicate lower K_D/K_i values with higher affinities for the tested protein, while lighter shades indicate lower affinities with higher K_D/K_i values. The gray sections indicate values not measured.

piperidine mixture yielded **47**. The benzoate groups were removed using sodium methoxide in a MeOH/THF mixture, and deprotection of primary alcohols was conducted in a HF-Py/pyridine/TMSOMe mixture to yield **49**. The free hydroxyls of **49** were sulfated by treatment with the pyridine–sulfur trioxide complex, and the resulting compound was saponified with LiOH in water to yield **51**. The azido and benzyl groups were subsequently reduced using Pd(OH)₂ followed by sulfation of the amino groups using the pyridine–sulfur trioxide complex in the presence of aqueous NaHCO₃/Na₂CO₃. Target molecule **3** was finally obtained after gel filtration and Sephadex LH-20 column purification.

The structures of 1–3 were analyzed and supported by one- and two-dimensional NMR experiments together with high resolution ESI-MS measurements (see the Supporting Information).

Heparin Binding Protein Affinity Results. The effect of the chemical pattern imprinted on these hexamers on their affinity for various HBPs was assessed by surface plasmon resonance (SPR) assays. Affinity-in-solution assays were designed to monitor the formation and interactions of oligosaccharide–protein complexes and determine the affinity of the interaction between the hexasaccharides and different heparin binding proteins. In addition, a specific inhibition format assay was used to determine the ability of molecules to disrupt the interaction between platelet selectin (PSEL) and platelet selectin glycoprotein ligand 1 (PSGL1).

We selected a group of seven growth factors (FGF1, FGF2, FGF4, FGF7, HBEGF, VEGF, and PDGFBB), one adhesion protein (PSEL), two cytokines (IL23 and IFN γ), six chemokines (CCL2, CCL5, CCL11, CXCL2, CXCL4, and CXCL12), and six differentiation proteins (BMP2, BMP4, BMP6, sFRP1, Shh, and WNT3A) for screening in the SPR assay. The results from this analysis are depicted in Figure 2. The affinity constants (K_D values) for each saccharide–protein interaction are listed in Table 1. The selection of our chosen protein panel was driven by the theorized involvement of the individual groups in cancer biology, including tumor angiogenesis (growth factors), tumor metastasis and invasion (PSEL), immunomodulation (cytokines), inflammation/leukocyte migration (chemokines), and oncogenesis (differentiation proteins).

The binding ability of the synthetic hexamers was compared to controls such as unfractionated heparin (UFH), enoxaparin, a hexamer fraction pool isolated from enoxaparin, and Fondaparinux, a synthetic pentasaccharide. As expected, all the hexamers that were tested typically exhibited affinities for HBPs 10–1000-fold lower than that of the larger enoxaparin and UFH but similar or slightly higher than that of Fondaparinux (data not reported). Over the course of this study, we chose to compare the binding data of the synthetic oligomers with those of the heterogeneous enoxaparin hexamer pool that was observed to exhibit either higher or equivalent affinity values, rather than Fondaparinux in the assays tested. In general, the synthetic hexasaccharides exhibited a range of

Table 1. *In Vitro* Affinity and/or Inhibition of the Hexasaccharide–HBP Interactions Tested^a

HBP	K_D (μM)			
	enoxaparin hexamer	1	2	3
VEGF165	14	66	86	14
PDGFBB	25000 ^b	25000 ^b	25000 ^b	25000 ^b
HBEGF	2	25000 ^b	25000 ^b	25000 ^b
FGF7	25000 ^b	25000 ^b	25000 ^b	25000 ^b
FGF4	25000 ^b	25000 ^b	25000 ^b	25000 ^b
FGF2	0.1	25000 ^b	1	25000 ^b
FGF1	0.3	25000 ^b	8	25000 ^b
PSEL/PSGL1	97	250	358	96
IL23	25000 ^b	25000 ^b	7	4
IFN γ	12	25000 ^b	10	7
CXCL12	250000 ^b	77	250000 ^b	24
CXCL4	25000 ^b	25000 ^b	25000 ^b	3
CXCL2	250000 ^b	250000 ^b	250000 ^b	250000 ^b
CCL11	25000 ^b	25000 ^b	25000 ^b	11
CCL5	25000 ^b	25000 ^b	25000 ^b	25000 ^b
CCL2	39	250000 ^b	250000 ^b	61
WNT3A	NT ^c	250000 ^b	250000 ^b	18
Shh	111	27	122	23
sFRP1	250000 ^b	250000 ^b	9	250000 ^b
BMP6	NT ^c	250000 ^b	250000 ^b	9
BMP4	250000 ^b	250000 ^b	250000 ^b	250000 ^b
BMP2	250000 ^b	24	46	34

^aIt should be noted that the measurements shown were derived from only one set of binding curves. ^bAbove the maximum for the given assay. ^cNot tested.

affinities similar to that of the enoxaparin hexamer pool for most of the HBPs tested, the exceptions being FGF1, FGF2, and HBEGF (Table 1). Among the 22 proteins tested, eight (BMP4, CCL5, CCL11, CXCL2, FGF4, FGF7, HBEGF, and PDGFBB) exhibited very low affinities for all synthetic hexamers, which could not be assessed by the SPR assay.

Binding preferences for individual proteins differed between the synthetic hexamers. Compound 1 exhibited the lowest affinity for any of the heparin-binding proteins (with the exception of Shh), consistent with prevalent literature suggesting that the *N*-sulfate groups are critical for these interactions. In the case of Shh, it was observed that 1 exhibited an affinity similar to that of 3 but an affinity increase of 4-fold compared to that of 2. This lower affinity of 2 was attributed to the absence of 6-*O*-sulfates, which is in accordance with literature reports.³²

Compound 2 exhibited an affinity higher than those of the other hexamers for FGF1, FGF2, and sFRP1. This compound was noticeably different from the other two compounds, because it completely lacked 6-*O*-sulfate groups but possessed three *N*-sulfated glucosamine residues. This is in concordance with previously reported data¹⁷ that the presence of *N*-sulfates was requisite as compared to 6-*O*-sulfates in the interaction of heparins with FGF2. Little about the interactions between sFRP1 and heparin has been published other than a report³³ postulating that 2-*O*-sulfation in heparin was critical for the interaction, which is consistent with our results.

Among the three hexasaccharides tested, irregular α -pentyl hexasaccharide 3 exhibited the highest affinity for BMP6, CCL2, CXCL12, CXCL4, IFN γ , IL23, PSEL/PSGL1, VEGF, and WNT3A. This set largely consists of proteins in the immunomodulatory/inflammation category. Interestingly, 3,

which has a backbone and charge density similar to 1 (with the exception of the internal disaccharide possessing an *N*-sulfate and 2-*OH* instead of a -*N*Ac/2-*OS* moiety), exhibited fairly higher affinities (\sim 2–6-fold increase) for the tested proteins, as compared to the latter, suggesting that molecular recognition definitely plays a significant role.

A closer examination of the synthetic hexamer binding relative to the size-fractionated enoxaparin hexamer yielded additional insights and supported the hypothesis that specific heparin sequences exhibit affinities for certain heparin binding proteins higher than that of the overall mixture. Specific synthetic heparins exhibited affinities for proteins BMP2, CXCL12, Shh, and CXCL4 higher than that of the enoxaparin hexamer fraction (Table 1). All three compounds (1–3) exhibited an affinity for BMP2 higher than that of the hexamer fraction, even though there was no significant preference observed within the group. In contrast, both 1 and 3 displayed \sim 4-fold increased affinity for Shh compared to that of 2 and the enoxaparin hexamer pool. However, only 3 exhibited an affinity for CXCL4 and CXCL12 substantially higher than those of the others, as shown in Figure 2. This clearly indicates that the structural pattern plays a role in *in vitro* potency, although no clear trend emerged from the analogues studied.

In general, the data obtained showed that the synthetic oligosaccharides could interact with several growth factors and chemokine sets implicated in different disease biologies. Although no obvious trend emerged from the three hexasaccharides tested, it was clear that the sulfation pattern influenced their affinities and potentially inhibitory activities significantly. Despite all three hexasaccharides possessing six overall sulfates, the variation in the placement of the sulfate groups was observed to undeniably influence the binding profiles of three hexasaccharides. For example, the interesting binding profile of 3, which possesses two *N*-acetyl glucosamines at the terminal end and an internal iduronic acid-*N*-sulfated glucosamine disaccharide and can be considered a hybrid of 1 (having *N*-acetyl glucosamines) and 2 (having *N*-sulfated glucosamines), may be attributed to its atypical conformational orientation as compared to those of the other two hexamers.

This study also suggests that apart from the typically studied oligosaccharides with repeating disaccharide structures, synthetic approaches afford the ability to make transition or unusual domains that may elicit a varied ability to engage with different subsets of target heparin binding proteins. It was inferred that comparing the hexamers to different heparin-like molecules other than unfractionated heparin might identify specific structural requirements that affect binding between HBPs and synthetic heparin-like molecules. This may allow further identification of potential oligosaccharide probes (or drugs) that could have selective activity in certain specific biological areas.

STD NMR. Saturation transfer difference (STD) NMR has recently emerged as a powerful tool for SAR studies, for screening synthetic ligand compound libraries for their binding to proteins and for determining the binding epitopes of the ligands.³⁴ In STD experiments, the magnetic saturation is initiated in the target protein and is transferred to the ligand protons in the proximity of the binding sites. The binding epitope of the ligands can therefore be mapped by accessing those saturations.

The three hexasaccharides were analyzed by STD NMR in an attempt to map or study the binding activity of the saccharides against FGF2. FGF2 was chosen as the target protein because

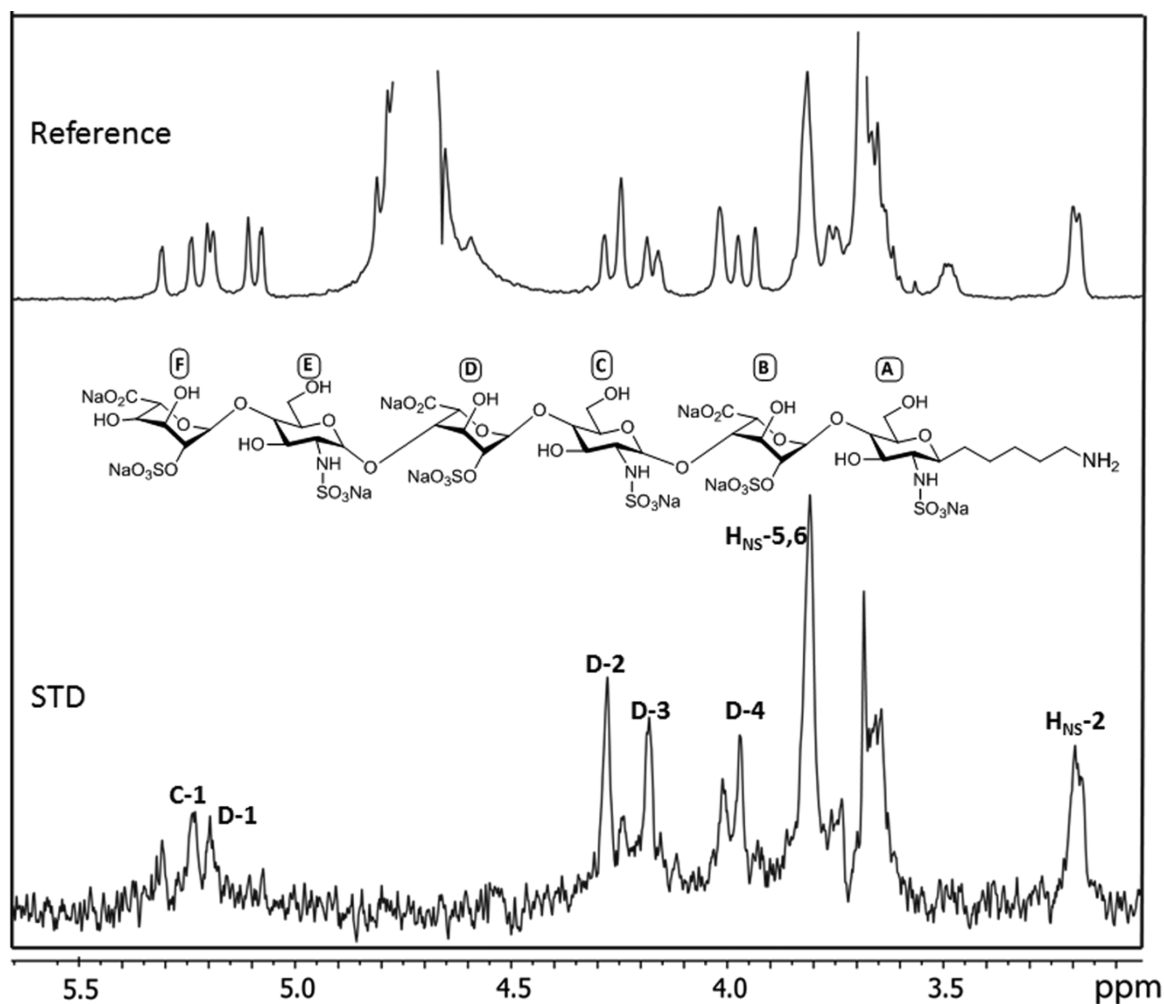


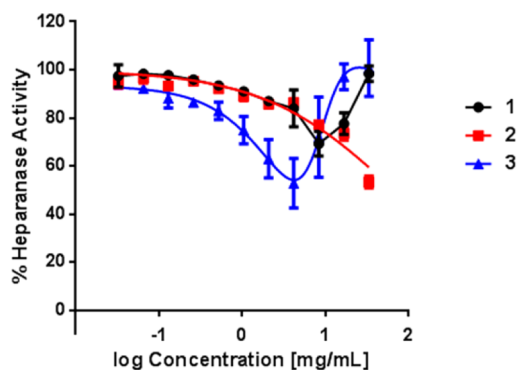
Figure 3. STD spectrum for hexasaccharide 2 complexed with FGF2.

of extensive studies published previously on FGF2–heparin oligosaccharide interactions^{17,35} and reported along with the X-ray crystallography³⁶ of the heparin–FGF2 complex.

Although weak STD signals were observed for both hexasaccharides 1 and 3, the STD spectrum shows no preferentially enhanced signals compared to the reference ¹H spectrum, which suggested the manifestation of nonspecific interactions between the hexamers and FGF2. On the other hand, the STD spectrum for 2 showed noticeable preferential enhancement of residue D, especially the H-2 resonance, indicating the 2-*O*-sulfate of residue D plays an essential role in its binding to FGF2 (Figure 3). Enhancement was also observed for glucosamine residue C adjacent to residue D as shown in Figure 3. This reasonably established the internal disaccharide sequence “C-D” in hexasaccharide 2 as the binding epitope in the oligomer–FGF2 interaction. STD NMR thus provides an elegant tool for gleaning information about the SAR of heparin oligosaccharides by probing the specific epitope mapping and/or interactions of oligosaccharides with different proteins.³⁷

Heparanase Inhibition Results. All three hexasaccharides were assessed for heparanase inhibition using an HTR-FRET assay. Remarkably, only 2 showed a typical heparanase inhibition profile with a calculated IC₅₀ value of 66.4 mg/mL, consistent with other LMWHs and Fondaparinux (data not shown). However, hexasaccharides 1 and 3 showed atypical

bell-shaped inhibition curves, which to the best of our knowledge have not been reported for heparins. It was unclear whether this unusual profile curve reflected a different mechanism of action or could be attributed to substrate competition at higher concentrations. As shown in Figure 4, compound 3 showed an inhibitory activity profile stronger than that of 1, exhibiting ~47% maximal inhibition at 4.2 mg/mL and ~31% maximal inhibition at 8.3 mg/mL. Both 1 and 2 showed similar inhibition profiles at concentrations ranging from 0.03 to 8 mg/mL, but their profiles diverged at higher concentrations. Both of these hexasaccharides possess similar 2-*O*-sulfations but differ in their *N*-substitution patterns, with 1 having only *N*-acetylated glucosamines as compared to all *N*-sulfated building blocks in 2. This indicates that the *N*-sulfates seem to contribute significantly to heparanase inhibition at higher concentrations. Interestingly, 3 showed more potent heparanase inhibition than 1 and 2 up to a concentration of 4 mg/mL, followed by decreased inhibitory activity with increasing concentrations. The data suggested that weaker 2-*O*-sulfation may facilitate heparanase inhibition, but that strong *N*-sulfation was essential for continued heparanase inhibition at higher concentrations. It may be possible that more sulfated compounds exhibit an inhibition mechanism different from that of their less sulfated counterparts, or there might be a size dependence that needs to be explored further. Though all three hexasaccharides tested show weak inhibition of heparanase



IC₅₀ Calculations:

- 1: N/A (30.7% max. inhibition at 8.3 mg/mL)
- 2: 66.39 mg/mL
- 3: N/A (47.2% max. inhibition at 4.2 mg/mL)

Figure 4. Dose-dependent heparanase inhibition by hexasaccharides 1–3.

activity, the observed patterns are intriguing. Testing of additional hexasaccharides or higher-order oligosaccharides with mixed 2-*O*-sulfation and full *N*-sulfation patterns would be a logical next step in further elucidating the mechanism of action and SAR for heparanase binding and inhibition.

CONCLUSIONS

A practical, concise route for the synthesis of three hexasaccharides, including the challenging synthesis of an irregular *N*-differentiated hexasaccharide, has been presented. Screening the three hexasaccharides through a series of *in vitro* protein binding and inhibition assays presented an unexpected SAR pattern, despite their analogous structures and similar charge densities. A positive correlation was observed between the observed 10-fold increase in FGF2 binding affinity for the hexasaccharide 2 and the distinct signal enhancements observed in the STD NMR in comparison to those of the other two hexamers. As a result, the specific binding epitope in 2 involved in the protein interaction was mapped using this technique. This has the potential to be used as a valuable tool for mapping out protein–saccharide interactions for future library screenings. Moreover, we also report here for the first time, to the best of our knowledge, the unusual bell-shaped heparanase inhibition curve of the irregular hexasaccharide 3, which calls for further probing into its mechanisms and implications. Predictably, 1 showed the lowest affinity for the panel of 22 HBPs tested as well as the weakest heparanase inhibition, emphasizing the importance of *N*-sulfates in these specific interactions.

The ability to synthesize discrete saccharide sequences allows for an enhanced assessment of the impact of subtle structural modifications that may not be easily accessible through the isolation of the more abundant structural motifs in HSGAGs. Our limited study, therefore, highlights the importance of using synthetic methodologies to meaningfully probe the structural space of HS, further leading to an elucidation of specific HS–protein interactions. Furthermore, the information can be used to design further compounds with potentially higher affinities and promising pharmaceutical candidates.

EXPERIMENTAL SECTION

All reactions were conducted under an atmosphere of nitrogen unless stated otherwise. All compounds were homogeneous as determined by thin layer chromatography (TLC) and had spectral properties consistent with their assigned structures. Purifications in organic solvents were performed by flash column chromatography on a Merck cartridge (GX0171511110LK [554-3646]; EVFD17, Si60, 15–40 μ m; 10 g) using the Isolera flash purification system (Biotage). Gel permeation chromatography with aqueous eluents was performed using Sephadex G-25 (GE Healthcare). Gel filtration chromatography with DMF or aqueous methanol as the eluent was performed using Sephadex LH-20. The compound purity was checked by TLC on silica gel 60 F254 (E. Merck) with detection by charring with sulfuric acid. The chemical purity of all compounds was determined by HPLC and ESI-TOF or LC–MS and confirmed to be $\geq 95\%$. ¹H NMR spectra were recorded on a Bruker 400 MHz instrument; chemical shifts were expressed relative to an internal tetramethylsilane (TMS; spectra recorded in organic solvents) or trimethylsilyl propionate (TSP; spectra recorded in D₂O) standard unless stated otherwise. MS analyses were performed on a Q-TOF QSTAR instrument (Applied Biosystems Inc.; *R* = 10000) and an FT-ICR instrument (7T Apex Bruker; *R* = 1000000). Before analysis in D₂O, samples were passed through a Chelex (Bio-Rad) ion exchange column and lyophilized three times from D₂O.

General Method for *O*-Glycosylation. In a dry round-bottom flask, the saccharide donor (1.3 equiv) and the saccharide acceptor (1 equiv) were dissolved in anhydrous toluene (0.2–0.4 M per acceptor) under a nitrogen atmosphere containing 4 Å molecular sieves (1 weight equivalent) previously activated at 400 °C. After being stirred for 30 min at room temperature, the solution was cooled to –20 °C, and a freshly prepared 0.1 M solution of *tert*-butyldimethylsilyl trifluoromethanesulfonate in toluene (0.2 equiv vs donor) was added dropwise. The reaction mixture was warmed from –20 to 0 °C over 30 min and stirred at this temperature for 1 h. The reaction mixture was neutralized with Et₃N until the pH reached 7, filtered through a pad of Celite, and concentrated to dryness under reduced pressure. The residue was purified by chromatography on a silica gel column to afford the glycosylated compound.

General Method for Isopropylidene Cleavage. The saccharide was dissolved in a 1/1 tetrahydrofuran/60% acetic acid mixture in water (0.16 M) at room temperature. The reaction mixture was stirred at 80 °C until complete conversion had been achieved. The reaction mixture was concentrated under reduced pressure and coevaporated with toluene. The residue was dissolved in dichloromethane and successively washed with a saturated aqueous solution of NaHCO₃ and a brine solution. The organic layer was dried over MgSO₄, filtered, and concentrated under reduced pressure to afford the crude compound.

General Method for Oxidation. To a solution of 0.015 M saccharide in an acetonitrile/saturated aqueous NaHCO₃ (50/50) mixture at room temperature were added TEMPO (0.1 equiv) and 1, 3-dibromo-5,5-dimethylhydantoin (2 equiv). The reaction mixture was stirred for 2 h at room temperature, after which a 1 M aqueous solution of Na₂S₂O₃ (to neutralize the 1,3-dibromo-5,5-dimethylhydantoin reagent) and ethyl acetate were added. The reaction mixture was cooled to 0 °C, and an aqueous solution of 1 M H₂SO₄ was added. The organic layer was separated, and the aqueous layer was extracted with ethyl acetate. The organic layers were combined, dried over MgSO₄, filtered, and concentrated under reduced pressure to give the intermediate carboxylic acid that was directly used in the next step without any further purification.

General Method for Esterification. To a solution of carboxylic acid in anhydrous DMF (0.1 M) under a nitrogen atmosphere was added iodomethane (10 equiv) followed by solid NaHCO₃ (10 equiv). The reaction mixture was stirred overnight at room temperature. The reaction mixture was diluted with ethyl acetate and successively washed with an aqueous solution of Na₂S₂O₃ (1 M), a brine solution, and water. The organic layer was dried over MgSO₄, filtered, and concentrated under reduced pressure, and the residue was purified by chromatography on a silica gel column to give the desired compound.

General Method for Selective Azide Reduction. The azido compound was dissolved in anhydrous methanol (0.02 M) under a nitrogen atmosphere. 1,3-Propanedithiol (10 equiv per N₃ function) and Et₃N (10 equiv per N₃ function) were successively added. The reaction mixture was protected from light and stirred for 2 days at room temperature or 40 °C. The reaction mixture was concentrated to dryness under reduced pressure, and the residue was purified by chromatography on a silica gel column or by a Sephadex LH20 gel column to afford the desired product.

Surface Plasmon Resonance Assays. Surface plasmon resonance (SPR) affinity-in-solution assays were conducted at 25 °C on either a ProteOn XPR36 instrument (Bio-Rad, Hercules, CA) or a Biacore T200 instrument (GE Healthcare, Piscataway, NJ). All recombinant human heparin-binding proteins were purchased from R&D Systems (Minneapolis, MN) with the exception of CXCL4 (PF4), which was purchased from Peprotech. All affinity-in-solution assays were conducted using methods adapted from the general format described by Karlsson.⁸

Assays conducted on the Biacore T200 chip were prepared in the same manner described previously.⁸ For assays on the ProteOn XPR36 instrument, a ProteOn NLC chip was loaded into the instrument, normalized, and conditioned with four 30 s injections of 50 mM sodium hydroxide. Neutravidin (Pierce Biotechnology, Rockford, IL) was immobilized on the reference and sample flow cells, and biotinylated low-molecular weight heparin was subsequently captured only on the sample flow cell. The heparin binding proteins at varying concentrations were mixed with a dilution series of each hexasaccharide sample and passed over the sensor chip (see Supporting Information). All data were single reference subtracted using the sensor chip interspot for each flow channel. A quadratic curve was used to fit slope versus concentration data for the standard curve. The free concentration of the protein in each test sample was calculated from the standard curve. The K_D (affinity constant) was calculated by the following equation:

$$K_D \text{ or } EC_{50} = ([P_{\text{free}}][H_{\text{total}}])/[P_{\text{bound}}]$$

where [P] is the protein concentration in molar units and [H] is the hexasaccharide concentration in mass per volume units. The reported value is the average K_D calculated at three hexasaccharide concentrations.

Inhibition of the PSEL/PSGL1 interaction by the hexasaccharide molecules was assessed by an inhibition assay.⁸ A dilution series of each hexasaccharide was mixed with 50 nM PSEL (R&D Systems). Each mixture was passed over the sensor surface coated with the PSGL1-Fc fusion protein (R&D Systems), and the response at equilibrium was measured. The IC₅₀ was calculated from the equilibrium response versus concentration data by nonlinear regression in GraphPad Prism. The constant of inhibition (K_i) was calculated from the IC₅₀ using the Cheng–Prusoff equation.

Heparanase Activity. Heparanase activity was measured using CisBio Bioassays technology based on time-resolved fluorescence energy transfer (TR-FRET) between europium cryptate and XL665 (allophycocyanin). The recombinant heparanase was preincubated with different concentrations of the heparin-derived compounds for 15 min at 37 °C prior to being added to the biotin-cryptate-labeled heparan sulfate substrate and incubated with streptavidin-XL665 for 1 h at 37 °C.

STD NMR. Recombinant human FGF2 was purchased from R&D Systems. The hexamer–FGF2 sample was prepared as 3.9 μM FGF2 and 780 μM heparin hexamer in 200 μL of PBS in D₂O (pH 6.5). NMR experiments were performed at 25 °C with a Bruker Avance 600 MHz spectrometer equipped with a QCI cryoprobe. STD NMR was acquired by using the Biospin sequence stddiff.3 with spin lock for protein signal suppression. The selective saturation was achieved by a train of Gauss-shaped pulses with a length of 50 ms, and the number of scans was 1280.

■ ASSOCIATED CONTENT

📄 Supporting Information

Detailed experimental procedures and spectral data for relevant compounds. This material is available free of charge via the Internet at <http://pubs.acs.org>.

■ AUTHOR INFORMATION

Corresponding Author

*E-mail: ganesh@momentapharma.com. Phone: (617) 491-9700. Fax: (617) 621-0431.

Author Contributions

S. Roy and A.E.H. contributed equally to this work.

Notes

The authors declare the following competing financial interest(s): A.E.H., S. Richard, F.D., and M.P. conducted the experimental work as part of a research project funded by Momenta Pharmaceuticals Inc. S. Roy, K.H., J.D., F.Y., Z.G.-G., I.C., and G.V.K. are employees of Momenta Pharmaceuticals Inc.

■ ACKNOWLEDGMENTS

We thank Dr. John Schaeck and Paul Miller for critical reading of the manuscript.

■ ABBREVIATIONS

FGF1, fibroblast growth factor 1; FGF2, fibroblast growth factor 2; FGF4, fibroblast growth factor 4; FGF7, fibroblast growth factor 7; HBEGF, heparin-binding epidermal growth factor; VEGF, vascular endothelial growth factor; PDGF, platelet-derived growth factor; PSEL, P-selectin; IL23, interleukin 23; IFN γ , interferon γ ; CCL2, CC chemokine ligand 2; CCL5, CC chemokine ligand 5; CCL11, CC chemokine ligand 11; CXCL2, CXC chemokine ligand 2; CXCL4, CXC chemokine ligand 24; CXCL12, CXC chemokine ligand 12; BMP2, bone morphogenetic protein 2; BMP4, bone morphogenetic protein 4; BMP6, bone morphogenetic protein 6; sFRP1, secreted frizzled related protein 1; Shh, sonic hedgehog; WNT3A, wingless-type MMTV integration site 3A; DMF, *N,N*-dimethylformamide; Et₃N, triethylamine; TEMPO, 2,2,6,6-tetramethylpiperidin-1-oxyl; DMAP, 4-dimethylaminopyridine; EDAC, *N*-(3-dimethylaminopropyl)-*N'*-ethylcarbodiimide hydrochloride; TBDPS, *tert*-butyldiphenylsilyl; TBDMS, *tert*-butyldimethylsilyl; Bn, benzyl; Ph, phenyl; Bz, benzoyl; PMB, *p*-methoxybenzyl; Me, methyl; Ac, acetate; Lev, levulinoyl; Cbz, benzyloxycarbonyl; Fmoc, fluorenylmethoxycarbonyl; NIS, *N*-iodosuccinimide; TfOH, trifluoromethanesulfonic acid; CSA, camphorsulfonic acid; Py-SO₃, pyridine–sulfur trioxide; BAIB, β -aminoisobutyric acid

■ REFERENCES

- (1) Hirsh, J.; Anand, S. S.; Halperin, J. L.; Fuster, V. Guide to anticoagulant therapy: Heparin: A statement for healthcare professionals from the American Heart Association. *Circulation* **2001**, *103*, 2994–3018.
- (2) Casu, B.; Vlodavsky, I.; Sanderson, R. D. Non anti-coagulant heparins and inhibition of cancer. *Pathophysiol. Haemostasis Thromb.* **2007**, *36*, 195–203.
- (3) Tyrrell, D. J.; Horne, A. P.; Holme, K. R.; Preuss, J. M.; Page, C. P. Heparin in inflammation: Potential therapeutic applications beyond anticoagulation. *Adv. Pharmacol.* **1999**, *46*, 151–208.
- (4) Bergamaschini, L.; Donarini, C.; Rossi, E.; De Luigi, A.; Vergani, C.; De Simon, M. G. Heparin attenuates cytotoxic and inflammatory

activity of Alzheimer amyloid- β *in vitro*. *Neurobiol. Aging* **2002**, *23*, 531–536.

(5) Lin, Y.-L.; Lei, H.-Y.; Lin, Y.-S.; Yeh, T.-M.; Chen, S.-H.; Liu, H.-S. Heparin inhibits dengue-2 virus infection of five human liver cell lines. *Antiviral Res.* **2002**, *56*, 93–96.

(6) Esko, J. D. Glycosaminoglycan binding proteins. In *Essentials of Glycobiology*; Varki, A., Ed.; Cold Spring Harbor Laboratory Press: Plainview, NY, 1999.

(7) Powell, A. K.; Yates, E. A.; Fernig, D. G.; Turnbull, J. E. Interactions of heparin/heparan sulfate with proteins: Appraisal of structural factors and experimental approaches. *Glycobiology* **2004**, *14*, 17R–30R.

(8) Roy, S.; Lai, H.; Zouaoui, R.; Duffner, J.; Zhou, H.; Jayaraman, L. P.; Zhao, G.; Ganguly, T.; Kishimoto, T. K.; Venkataraman, G. Bioactivity screening of partially desulfated low-molecular weight heparins: A structure/activity relationship study. *Glycobiology* **2011**, *21*, 1194–1205.

(9) Faham, S.; Hileman, R. E.; Fromm, J. R.; Linhardt, R. J.; Rees, D. C. Heparin structure and interactions with basic fibroblast growth factor. *Science* **1996**, *271*, 1116–1120.

(10) DiGabriele, A. D.; Lax, I.; Chen, D. I.; Svahn, C. M.; Jaye, M.; Schlessinger, J.; Hendrickson, W. A. Structure of a heparin-linked biologically active dimer of fibroblast growth factor. *Nature* **1998**, *393*, 812–817.

(11) Zhao, W.; McCallum, S. A.; Xiao, Z.; Zhang, F.; Linhardt, R. J. Binding affinities of vascular endothelial growth factor (VEGF) for heparin-derived oligosaccharides. *Biosci. Rep.* **2012**, *32*, 71–81.

(12) Hostettler, N.; Naggi, A.; Torri, G.; Casu, B.; Vlodaysky, I.; Borsig, L. P-Selectin- and heparanase-dependent antimetastatic activity of non-anticoagulant heparins. *FASEB J.* **2007**, *21*, 3562–3572.

(13) Liu, J.; Shriver, Z.; Pope, R. M.; Thorp, S. C.; Duncan, M. B.; Copeland, R. J.; Raska, C. S.; Yoshida, K.; Eisenberg, R. J.; Cohen, G.; Linhardt, R. J.; Sasisekharan, R. C. Characterization of a heparan sulfate octasaccharide that binds to *Herpes simplex* virus type 1 glycoprotein D. *J. Biol. Chem.* **2002**, *277*, 33456–33467.

(14) Fry, E. E.; Lea, S. M.; Jackson, T.; Newman, J. W.; Ellard, F. M.; Blakemore, W. E.; Abu-Ghazaleh, R.; Samuel, A.; King, A. M.; Stuart, D. I. The structure and function of a foot-and-mouth disease virus-oligosaccharide receptor complex. *EMBO J.* **1999**, *18*, 543–554.

(15) Petitou, M.; van Boeckel, C. A. A synthetic antithrombin III binding pentasaccharide is now a drug! What comes next? *Angew. Chem., Int. Ed.* **2004**, *42*, 3118–3133.

(16) Schwörer, R.; Zubkova, O. V.; Turnbull, J. E.; Tyler, P. C. Synthesis of a targeted library of heparan sulfate hexa- to dodecasaccharides as inhibitors of β -secretase: Potential therapeutics for Alzheimer's disease. *Chem.—Eur. J.* **2013**, *19*, 6817–6823.

(17) Noti, C.; de Paz, J. L.; Polito, L.; Seeberger, P. H. Preparation and use of microarrays containing synthetic heparin oligosaccharides for the rapid analysis of heparin–protein interactions. *Chem.—Eur. J.* **2006**, *12*, 8664–8686.

(18) Cabannes, E.; Caravano, A.; Lewandowski, D.; Motte, V.; Nancy-Portebois, V.; Petitou, M.; Pierdet, P. Oligosaccharide compounds for use in mobilizing stem cells. WO2010/29185 A1, 2010.

(19) Jacquinet, J.-C.; Petitou, M.; Duchaussoy, P.; Lederman, I.; Choay, J.; Torri, G.; Sinay, P. Synthesis of heparin fragments. A chemical synthesis of the trisaccharide O-(2-deoxy-2-sulfamido-3,6-di-O-sulfo- α -D-glucopyranosyl)-(1 \rightarrow 4)-O-(2-O-sulfo- α -L-idopyranosyluronic acid)-(1 \rightarrow 4)-2-deoxy-2-sulfamido-6-O-sulfo-D-glucopyranose heptasodium salt. *Carbohydr. Res.* **1984**, *130*, 221–242.

(20) Reinold, V. N.; Carr, S. A.; Green, B. N.; Petitou, M.; Choay, J.; Sinay, P. Structural characterization of sulfated glycosaminoglycans by fast atom bombardment mass spectrometry: Application to heparin fragments prepared by chemical synthesis. *Carbohydr. Res.* **1987**, *161*, 305–313.

(21) Jaurand, G.; Tabeur, C.; Petitou, M. Synthesis of the basic disaccharide unit of heparin. *Carbohydr. Res.* **1994**, *255*, 295–302.

(22) Petitou, M.; Duchaussoy, P.; Jaurand, G.; Gourvenec, F.; Lederman, I.; Strassel, J.-M.; Bâzru, T.; Crépon, B.; Hérault, J.-P.;

Lormeau, J.-C.; Bernat, A.; Herbert, J.-M. Synthesis and pharmacological properties of a close analogue of an antithrombotic pentasaccharide SR 90107A/ORG 31540. *J. Med. Chem.* **1997**, *40*, 1600–1607.

(23) Paz, J. L.; Martin-Lomas, M. Synthesis and biological evaluation of a heparin-like hexasaccharide with the structural motifs for binding to FGF and FGFR. *Eur. J. Org. Chem.* **2005**, *9*, 1849–1858.

(24) Lubineau, A.; Lortat-Jacob, H.; Gavard, O.; Sarrazin, S.; Bonnaffe, D. Synthesis of tailor-made glycoconjugate mimetics of heparan sulfate that bind IFN- γ in the nanomolar range. *Chem.—Eur. J.* **2004**, *10*, 4265–4282.

(25) Hu, Y.-P.; Lin, S.-Y.; Huang, C.-Y.; Zulueta, M. M. L.; Liu, J.-Y.; Chang, W.; Hung, S.-H. Synthesis of 3-O-sulfonated heparan sulfate octasaccharides that inhibit the *Herpes simplex* virus type 1 host-cell interaction. *Nat. Chem.* **2011**, *3*, 557–563.

(26) Hamza, D.; Lucas, R.; Feizi, T.; Chai, W.; Bonnaffe, D.; Lubineau, A. First synthesis of heparan sulfate tetrasaccharides containing both N-acetylated and N-unsubstituted glucosamine: Search for putative 10E4 epitopes. *ChemBioChem* **2006**, *7*, 1856–1858.

(27) Tabeur, C.; Mallet, J. M.; Bono, F.; Herbert, J. M.; Petitou, M.; Sinaÿ, P. Oligosaccharides corresponding to the regular sequence of heparin: Chemical synthesis and interaction with FGF-2. *Bioorg. Med. Chem.* **1999**, *7*, 2003–2012.

(28) Yin, J.; Seeberger, P. H. Applications of heparin and heparan sulfate microarrays. *Methods Enzymol.* **2010**, *478*, 197–218.

(29) Arungundram, S.; Al-Mafraji, K.; Asong, J.; Venot, A.; Boons, G.-J.; Leach, F. E., III; Amster, I. J.; Turnbull, J. E. Modular synthesis of heparan sulfate oligosaccharides for structure-activity relationship studies. *J. Am. Chem. Soc.* **2009**, *131*, 17394–17405.

(30) Boons, G.-J. Heparan sulfate synthesis. WO2010/117803 A2, 2010.

(31) Tabeur, C.; Machtetto, F.; Mallet, J.-M.; Duchaussoy, P.; Petitou, M.; Sinay, P. L-Iduronic acid derivatives as glycosyl donors. *Carbohydr. Res.* **1996**, *281*, 253–276.

(32) Zhang, F.; McLellan, J. S.; Ayala, A. M.; Leahy, D. J.; Linhardt, R. J. Kinetic and structural studies on interactions between heparin or heparan sulfate and proteins of the hedgehog signaling pathway. *Biochemistry* **2007**, *46*, 3933–3941.

(33) Zhong, X.; Desilva, T.; Lin, L.; Bodine, P.; Bhat, R. A.; Presman, E.; Pocas, J.; Stahl, M.; Kriz, R. Regulation of secreted frizzled-related protein-1 by heparin. *J. Biol. Chem.* **2007**, *282*, 20523–20533.

(34) Angulo, J.; Nieto, P. M. STD-NMR: Application to transient interactions between biomolecules—a quantitative approach. *Eur. Biophys. J.* **2011**, *40*, 1357–1369.

(35) Kreuger, J.; Salmivirta, M.; Sturiale, L.; Giménez-Gallego, G.; Lindahl, U. Sequence analysis of heparan sulfate epitopes with graded affinities for fibroblast growth factors 1 and 2. *J. Biol. Chem.* **2001**, *276*, 30744–30752.

(36) Faham, S.; Hileman, R. E.; Fromm, J. R.; Linhardt, R. J.; Rees, D. C. Heparin structure and interactions with basic fibroblast growth factor. *Science* **1996**, *271*, 1116–1120.

(37) Yu, F.; Roy, S.; Arevalo, E.; Schaeck, J.; Wang, J.; Holte, K.; Duffner, J.; Gunay, N. S.; Capila, I.; Kaundinya, G. V. Characterization of heparin-protein interaction by saturation transfer difference (STD) NMR. *Anal. Bioanal. Chem.* **2014**, *406*, 3079–3089.